

## Room-temperature Synthesis and Characterization of Ni-included Carbon Nanofibers

Z. P. Wang\*, D. Takeuchi, K. Yamaguchi, Y. Hayashi and M. Tanemura

Department of Environmental Technology, Graduate School of Engineering, Nagoya Institute of Technology, Gokiso-cho, Showa-ku, Nagoya 466-8555, JAPAN

Fax: 81-052-735-5379, e-mail: wangzhipeng11@gmail.com

**Abstract:** Graphite surfaces were sputtered by Ar<sup>+</sup> ions with and without a simultaneous Ni supply at room temperature. The sputtered surface without a Ni supply was covered with densely distributed conical protrusions and aligned single carbon nanofibers (CNFs) grew on the respective tips, whereas Ar<sup>+</sup>-sputtered surfaces with a simultaneous Ni supply were characterized by rod-like and nanofibrous structures, depending on the Ni content of the nanostructures. Pristine CNFs without a metal supply were characterized as the amorphous nature, while the Ni-included nanorods and CNFs were featured as polycrystalline nature and consisted of both carbon and Ni. Thus, the shape and crystalline structure of sputter-induced nanostructures were strongly affected by Ni supply. A field emission characteristic of Ni-included CNFs was also investigated.

**Key words:** carbon, nanofibers, nickel, ion beam, field emission

### 1. INTRODUCTION

Since the revolutionary discovery by Iijima<sup>[1]</sup> in 1991, carbon nanotubes (CNTs) and carbon nanofibers (CNFs) were investigated extensively by many researchers owing to their novel physical properties and various kinds of applications including a platform for gene delivery, catalyst supports in petrochemistry, composite materials, scanning probe microscopy tips and electron field emission sources<sup>[2-5]</sup>. They have been conventionally synthesized by arc discharge between two carbon electrodes<sup>[1]</sup>, laser ablation from a carbon target<sup>[6]</sup> and plasma enhanced chemical vapor deposition from carbon containing gaseous species<sup>[7]</sup>. However, in those conventional synthesis methods, the growth temperatures higher than 500°C are generally required for their growth. For their more widespread applications, this high-temperature requirement for the growth should be broken through.

In the previous papers, we demonstrated that Ar<sup>+</sup> ion irradiation to bulk carbon and carbon coated substrates induced formation of conical protrusions and single CNFs (pristine CNFs) pointing in the ion-beam direction grew on the cone top (CNF-tipped cones) without catalyst, even at room temperature<sup>[8-10]</sup>. The ion-induced CNFs thus synthesized, which were typically 20-50nm in diameter and micrometer range in length, showed good field emission (FE) properties. As is well-known, the FE properties are highly dependent on both the electrical properties and the shape of emitters. Consequently, metal incorporation into ion-induced CNFs will lead to a change in the electrical conductivity of CNFs and hence further improves the FE property. In the present work, as the first step of the detailed investigation of the metal supply effect on the FE

properties, we tackled Ni inclusion into CNFs during the ion-induced CNF growth at room temperature. The crystalline structure of CNFs including Ni was investigated in detail. In addition, the FE property of ion-induced CNFs with Ni supply was also measured.

### 2. EXPERIMENTAL DETAILS

The substrates employed were graphite sheets of 0.08 mm in thickness. They were bombarded by Ar<sup>+</sup> ions with and without Ni supply using Kaufman-type ion gun (Iontech. Inc. Ltd., model 3-1500-100FC). Since the oblique Ar<sup>+</sup> irradiation is more suitable for ion-induced CNF growth than sputtering at normal incidence<sup>[11]</sup>, the incident angle of the ion beam was set at 45° from the normal to the surface. For Ni supply, the Ni sheet, 10 mm in height, was mounted perpendicularly near the graphite sample, and they were co-sputtered by Ar<sup>+</sup> ions. The diameter and energy of the ion beam employed were 6 cm and 1 keV, respectively. The duration for the CNFs growth was 60 min. The basal and working pressures of the growth chamber were 1.5×10<sup>-5</sup>Pa and 2×10<sup>-2</sup>Pa, respectively.

After sputtering, the morphology of the sample surfaces and the crystalline structure of CNFs with and without Ni thus grown were investigated by scanning electron microscope [SEM (JEOL, JEM-5600)] and transmission electron microscope [TEM (JEOL, JEM-3010)], respectively. Because the graphite sheet is very thin, the CNFs-grown graphite sheets were directly mounted on a TEM sample holder without any post-treatment. The FE properties of the samples were measured in a JAMP-7100 scanning Auger microscope (SAM) under an ultra-high vacuum ambient.

### 3. RESULTS AND DISCUSSION

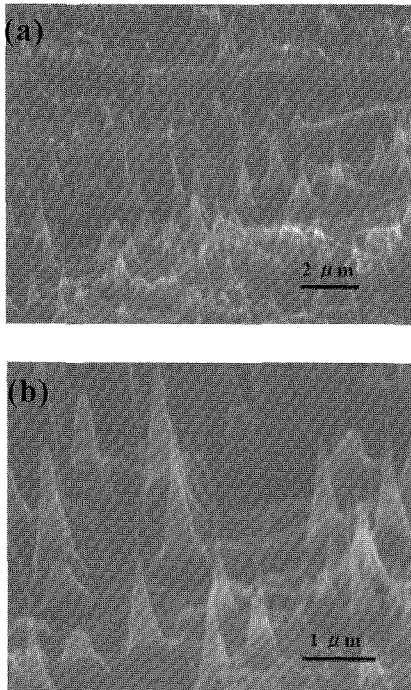


Fig. 1 (a) Typical SEM image of a graphite surface  $\text{Ar}^+$ -ion irradiated at 1keV without Ni supply for 60 min at room temperature. (b) High-magnification SEM image

Figure 1 shows SEM images of a sputtered graphite sheet surface without a simultaneous Ni supply, revealing that the whole surface of the graphite sheet was covered with uniformly distributed conical protrusions (500 nm in average diameter of the stem) and single pristine CNFs grew on the tops. Both of them were pointing in the incident direction of the ion beam.

Very interestingly, no CNF grew without cone bases and more than one CNF never grew on the respective cone tips [Fig.1 (b)]. The similar CNF-tipped cones were observed previously on the surfaces of bulk graphite and carbon-coated various kinds of substrates sputtered by  $\text{Ar}^+$  ions [8-10]. CNFs were 0.5-2  $\mu\text{m}$  in length, independent of the cone size. The apex angles of the basal cones on which CNFs grew were 17-25° (20° in average). It should be noted that most of the CNFs were located on the central axis of the cone. The growth mechanism of CNFs is the re-deposition of carbon atoms sputter-ejected from the surface onto the sidewall of the conical structures and the surface diffusion of the excess carbon atoms toward the tips during sputtering [8]. In this process, the surface diffusion of carbon atoms would play an important role in the formation of CNFs. In fact, growth rate of the ion-induced CNFs is known to depend on the sample temperature [11].

Figure 2 shows TEM images of a typical CNF-tipped-cone thus grown. In Figures 2(a), 2(b) and 2(c), no hollow structure was observed in the CNF, indicating that the CNF were different from CNTs. No clear boundary between the CNF and the cone was recognizable. Fig. 2(d) shows electron diffraction pattern (EDP) from the tip region of the CNF. The EDP was composed of the broad hallow ring, proving that the CNF was amorphous-like or of very fine crystalline nature. The result was consistent with that observed previously for ion-induced CNFs grown at room temperature on a carbon coated Ni mesh. Hofmann et al. also demonstrated that CNTs synthesized by plasma-enhanced CVD at 120°C were low in the graphitization quality [12]. Thus, the amorphous-like structure may be a feature common to carbon nanomaterials grown at low temperatures.

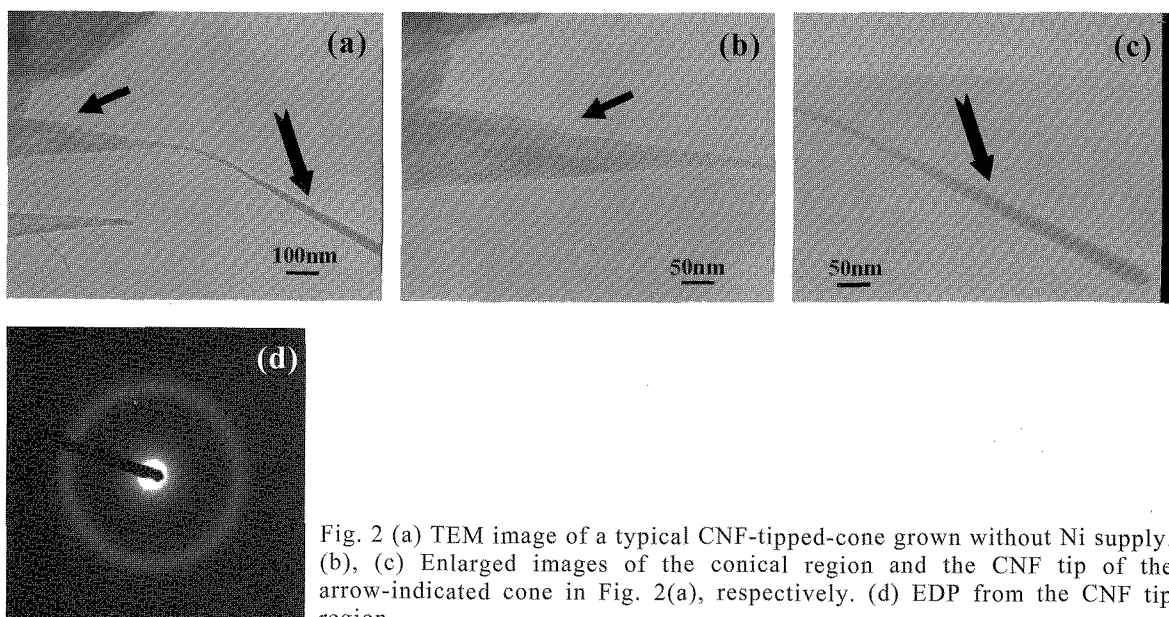


Fig. 2 (a) TEM image of a typical CNF-tipped-cone grown without Ni supply. (b), (c) Enlarged images of the conical region and the CNF tip of the arrow-indicated cone in Fig. 2(a), respectively. (d) EDP from the CNF tip region.

Figure 3 shows an SEM image of a typical graphite sheet surface sputtered with a simultaneous Ni supply. The sputtered surface was covered with nanorods, nanocones, and nanofiber-tipped nanocones. The length of the nanorods was less than 6  $\mu\text{m}$ , the diameter of the nanorods ranged from 30 to 400 nm. The length and the diameter of the nanofibers on the nanocones were 0.5-4  $\mu\text{m}$  and 20-50 nm, respectively. It must be noted that the nanocones without CNF formed on the surface sputtered with a Ni supply. As was described above, the surface diffusion of carbon is responsible for the CNF growth. Consequently, the supplied Ni may suppress the diffusion of carbon atoms, and hence fewer CNF growth on the nanocone top.

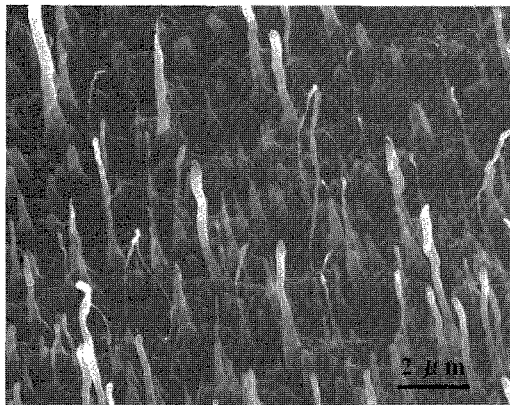


Fig. 3 SEM image of a graphite surface sputtered with a simultaneous Ni supply

Figure 4 shows TEM images of a tip region of a rod-like nanostructure and CNF-tipped-cones grown with a simultaneous Ni supply. Fig. 4(c) shows the corresponding EDP of the tip region of the rod-like nanostructure. The EDP indicated that the rod-like nanostructure was comprised of carbon and Ni atoms, and Ni atoms were included into the carbon nanostructures successfully. A typical TEM image of a Ni-included CNF grown on a cone was shown in Fig. 4(b). Similar to the pristine CNFs, no boundary between the CNF and the cone was recognizable. In addition, no hollow structure was observed, implying that it is fibrous, not tubular. Fig. 4(d) shows an EDP taken at the tip region of the CNF. The EDP consisted of spotty rings arising from Ni (111) or graphite (101) (the 1st inner ring) and Ni (200) (the 2nd inner ring). Thus, the CNF was characterized by the polycrystalline nature, and Ni was surely included in the CNF.

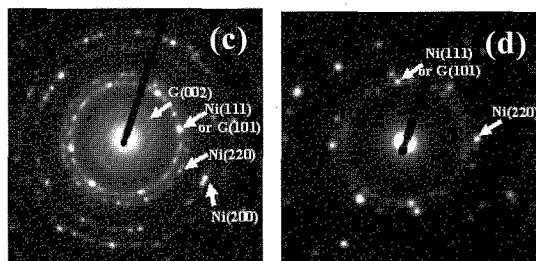
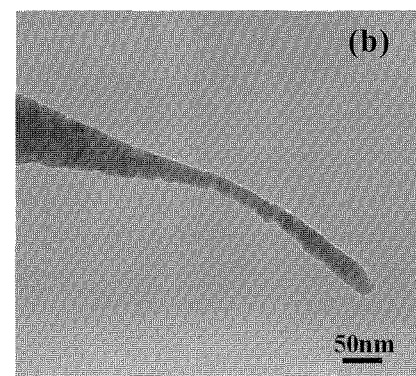
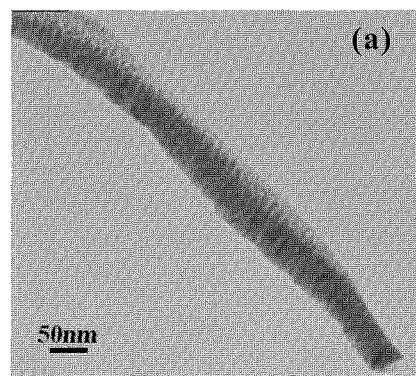


Fig. 4 (a) and (b) TEM images of rod-like nanostructure and Ni-included CNF grown on a cone, respectively. (c) and (d) EDPs from the tip regions of the nanorod and Ni-included CNF in Fig. 4 (a) and (b), respectively.

FE measurements were carried out with applied voltages from 0 to 2000 V in an ultra-high vacuum chamber operated at a base pressure of  $10^{-6}$  Pa. The distance between the cathode and the anode was kept at 200  $\mu\text{m}$ . Figure 5 shows the FE characteristics obtained for the surface of the graphite sheet sputtered with a Ni supply. The corresponding Fowler-Nordheim (FN) plot is also shown in the inset of Fig. 5. The current density  $J$  was calculated using the anode area ( $7.9 \times 10^{-3}$   $\text{cm}^2$ ). The threshold field, which we defined as the field required to generate an emission current density of  $1 \mu\text{A}/\text{cm}^2$ , was 3.0  $\text{V}/\mu\text{m}$  as shown in Fig. 5. This value was slightly better than that reported previously for ion-induced CNFs without metal supply, 3.65  $\text{V}/\mu\text{m}$  [13], and better than that obtained for CNTs grown at low temperature, 4.2  $\text{V}/\mu\text{m}$  [14]. From a viewpoint of the morphological factor for the better FE property, less number density of CNF-tipped cones for the surface sputtered with a Ni supply would be disadvantageous, compared with

CNFs grown on the surface sputtered without a Ni supply. Consequently, the observed slightly better FE property maybe owe to the better conductivity of Ni-included CNFs. In order to establish the firm conclusion, dependence of FE properties on the CNF conductivity should be investigated for single CNFs with various amount of Ni. Investigations along this line are now being undertaken.

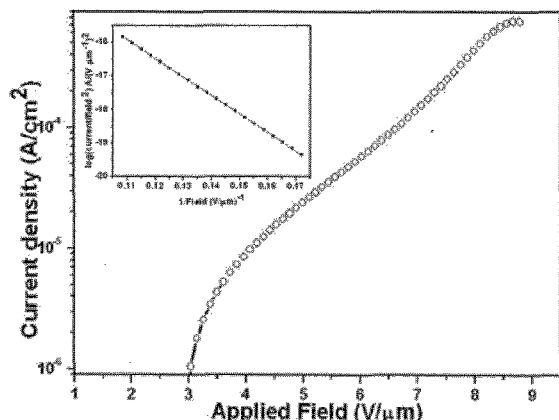


Fig. 5 Field emission characteristics for Ni-included CNFs. Inset: Corresponding FN plot

The corresponding Fowler-Nordheim (FN) plot is shown in the Fig.5, representing the linear behavior of the curve. Assuming a work function of 4.5 eV for the graphite, an effective field enhancement factor  $\beta$  calculated from the FN plot was  $\sim 1170$ , which is comparable with that reported for ion-induced CNFs grown on a graphite plate without a metal supply<sup>[8]</sup>.

#### 4. CONCLUSIONS

Graphite surfaces were sputtered by  $\text{Ar}^+$  ions with and without a simultaneous Ni supply at room temperature. The sputtered surface without Ni supply was covered with densely distributed CNF-tipped conical protrusions, whereas  $\text{Ar}^+$ -sputtered surfaces with a simultaneous Ni supply were characterized by nanorods, nanocones and nanofiber-tipped nanocones. Pristine CNFs were characterized by the amorphous-like nature, whereas the Ni-included CNFs were featured by polycrystalline structure. Ni-included CNFs were also demonstrated to be promising as field electron emitters.

#### ACKNOWLEDGMENTS

This work was partially supported by the Japan Society for the Promotion of Science (JSPS; Grants-in-Aid for Scientific Research B, No. 18360022).

#### REFERENCES

- [1] S. Iijima, *Nature*, **354**, 56(1991).
- [2] P. Poncharal, Z. L. Wang, D. Ugarte, W. A. de Heer, *Science*, **283**, 1513(1999).
- [3] R. H. Baughman, A. A. Zakhidov, W. A. de Heer, *Science*, **297**, 787(2002).
- [4] M. A. Guillorn, A. V. Melechko, V. I. Merkulov, D. K. Hensley, M. L. Simpson, D. H. Lowndes, *Appl.*

*Phys. Lett.*, **81**, 3660(2003).

- [5] M. Zhang, S. L. Fang, A. A. Zakhidov, S. B. Lee, A. E. Aliev, C. D. Williams, K. R. Atkinson, R. H. Baughman, *Science*, **309**, 1215(2005).
- [6] A. Thess, R. Lee, P. Nikolaev, H. J. Dai, P. Petit, J. Robert, C. H. Xu, Y. H. Lee, S. G. Kim, A. G. Rinzler, D. T. Colbert, G. E. Scuseria, D. Tomanek, J. E. Fischer, R. E. Smalley, *Science*, **273**, 483(1996).
- [7] Z. F. Ren, Z. P. Huang, J. W. Xu, J. H. Wang, P. Bush, M. P. Siegal, P. N. Provencio, *Science*, **282**, 1105(1998).
- [8] M. Tanemura, J. Tanaka, K. Itoh, Y. Fujimoto, Y. Agawa, L. Miao, S. Tanemura, *Appl. Phys. Lett.*, **86**, 113107(2005).
- [9] M. Tanemura, J. Tanaka, K. Itoh, T. Okita, L. Miao, S. Tanemura, S. P. Lau, L. Huang, Y. Agawa, M. Kitazawa, *Appl. Phys. Lett.*, **87**, 193102(2005).
- [10] M. Tanemura, H. Hatano, M. Kitazawa, J. Tanaka, T. Okita, S. P. Lau, H. Y. Yang, S. F. Yu, L. Huang, L. Miao, S. Tanemura, *Surface Science*, **600**, 3663(2006).
- [11] M. Tanemura, T. Okita, H. Yamauchi, S. Tanemura, R. Morishima, *Appl. Phys. Lett.*, **84**, 3831(2004).
- [12] S. Hofmann, C. Ducati, J. Robertson, B. Kleinsorge, *Appl. Phys. Lett.*, **83**, 135(2003).
- [13] H. S. Sim, S. P. Lau, H. Y. Yang, L. K. Ang, M. Tanemura, K. Yamaguchi, *Appl. Phys. Lett.*, **90**, 143103(2007).
- [14] S. Hofmann, C. Ducati, B. Kleinsorge, J. Robertson, *Appl. Phys. Lett.*, **83**, 4661(2003).

(Received January 8, 2008.; Accepted July 17, 2008)